

A Molecular Picture of Diffusion Controlled Reaction: Role of Microviscosity and Hydration on Hydrolysis of Benzoyl Chloride at a Polymer Hydration Region

Pramod Kumar Verma, Rajib Kumar Mitra, and Samir Kumar Pal*

*Unit for Nano Science & Technology Department of Chemical, Biological & Macromolecular Sciences, S.N. Bose National Center for Basic Sciences Block JD, Sector III, Salt Lake, Kolkata 700098, India**Received March 5, 2009. Revised Manuscript Received July 7, 2009*

In this study, we have attempted to explore the molecular mechanism associated with a diffusion controlled reaction at a polymer hydration region by monitoring temperature-dependent solvolysis reaction of benzoyl chloride (BzCl) in water–poly(ethylene glycol) mixture at low water concentration. BzCl being highly hydrophobic resides in the vicinity of the PEG surface and the reaction takes place at the interface. Temperature-dependent solvolysis allows one to estimate the overall Arrhenius type activation energy barrier associated with the reaction. To understand the relative contribution of hydration and diffusive motion on the overall activation energy we studied the temperature-dependent picosecond-resolved solvation dynamics using a fluorescence probe Coumarin 500 (C500). The observed acceleration of solvation dynamics with temperature finds its origin in temperature-induced transition of bound to free type interfacial water molecules near the PEG surface. Temperature-dependent acoustic and densimetric studies also support this phenomenon. The temperature-induced enhancement of the local viscosity experienced by the probe, which is calculated from the rotational anisotropy studies, furnishes the activation barrier for microviscosity as applicable to the Kramers model. The activation energy barriers estimated from the temperature-dependent solvation dynamics and microviscosity studies are correlated with that obtained from the solvolysis reaction.

Introduction

Most of the chemical reactions are multistep in nature and if one of the steps is diffusion controlled, the slow diffusion step generally serves as the rate determining one. An Arrhenius type of plot of the kinetics of the reaction provides information about the overall energy barrier of the reaction. However, for a multistep reaction, the barrier contains contributions from various steps involved, and to correlate the contribution from such steps to the total energy, we attempt to study a simple solvolysis reaction on a polymer hydration region, which has contributions from both the translational diffusion and the hydration. To the best of our understanding, a detailed picture of such a diffusion controlled reaction, which is useful in various fields of experimental condensed matter physics and synthetic chemistry,^{1,2} has not yet been explored to date, and that drives our motivation toward the present study.

As a model reaction occurring at a polymer hydration region, we spectroscopically monitor the kinetics of the solvolysis of benzoyl chloride (BzCl) at different temperatures in low concentration of water-in-PEG solution. In such a reaction, two important factors that govern the rate of the reaction are the activity of nucleophilic water molecules, i.e., the availability of free water molecules and the diffusion of the water molecules along the polymeric hydration region. It is to be noted that the activity of water molecules in polymer solution can be tuned by varying the concentration of the polymer.^{3,4} The study of the interaction between water and synthetic polymers, such as poly(2-methoxy-

ethyl acrylate) (PMEA), poly(*N*-vinyl-2-pyrrolidone) (PVP), and poly(ethylene glycol) (PEG), has been a key interest of research over the years.^{5–7} Vogler⁸ reviewed the structure of water at biomaterial surfaces and suggested the presence of two distinct kinds of water structures. Kitano and Tanaka et al.^{9,10} studied the structure of water absorbed in PMEa by FTIR spectroscopy and concluded the presence of nonfreezing water on the polymer surface which makes the PMEa an excellent blood compatible. Xu et al.¹¹ examined the diffusion and structure of water in PVP and its copolymers using FTIR technique to conclude the existence of three different types of water with different degrees of hydrogen bonding at the polymer water interface. The presence of these polymers significantly changes the local and long-range water structure network: an effect of outstanding importance in understanding many physicochemical and biological processes. The physicochemical behavior of PEG in aqueous solution remains puzzling¹² despite the proliferation of experimental studies involving conductometry,¹³ differential scanning calorimetry,¹⁴

(5) Tasaki, K. *J. Am. Chem. Soc.* **1996**, *118*, 8459–8469.(6) Kjellander, R.; Florin, E. *J. Chem. Soc., Faraday Trans. 1* **1981**, *77*, 2053–2077.(7) Bieze, T. W. N.; Barnes, A. C.; Huige, C. J. M.; Enderby, J. E.; Leyte, J. C. *J. Phys. Chem.* **1994**, *98*, 6568–6576.(8) Vogler, E. A. *Adv. Colloid Interface Sci.* **1998**, *74*, 69–117.(9) Ide, M.; Mori, T.; Ichikawa, K.; Kitano, H.; Tanaka, M.; Mochizuki, A.; Oshiyama, H.; Mizuno, W. *Langmuir* **2003**, *19*, 429–435.(10) Kitano, H.; Ichikawa, K.; Fukuda, M.; Mochizuki, A.; Tanaka, M. *J. Colloid Interface Sci.* **2001**, *242*, 133–140.(11) Wan, L.-S.; Huang, X.-J.; Xu, Z.-K. *J. Phys. Chem. B* **2007**, *111*, 922–928.(12) Faraone, A.; Magazù, S.; Maisano, G.; Migliardo, P.; Tettamanti, E.; Villari, V. *J. Chem. Phys.* **1999**, *110*, 1801–1806.(13) Bisal, S.; Bhattacharya, P. K.; Moulik, S. P. *J. Phys. Chem.* **1990**, *94*, 4212–4216.(14) Graham, N. B.; Zulfikar, M.; Nwachuku, N. E.; Rashid, A. *Polymer* **1989**, *30*, 528–533.(15) Derkaoui, N.; Said, S.; Grohens, Y.; Olier, R.; Privat, M. *J. Colloid Interface Sci.* **2007**, *305*, 330–338.

*Corresponding author. E-mail: skpal@bose.res.in.

(1) Clinton, N.; Matlock, P. *Encyclopedia of Polymers*; John Wiley & Sons: New York, 1986.(2) Harris, J. M. *Poly(Ethylene Glycol) Chemistry*; Plenum: New York, 1992.(3) Reid, C.; Rand, R. P. *Biophys. J.* **1997**, *72*, 1022–1030.(4) Völker, J.; Breslauer, K. J. *Annu. Rev. Biophys. Biomol. Struct.* **2005**, *34*, 21–42.

NMR,¹⁵ and acoustic and densimetric measurements^{16,17} as well as molecular dynamics simulation¹⁸ carried out at both macroscopic and microscopic levels.⁵ The hydration structure of the PEG chain is a fundamental factor for understanding its conformation and stability, since the hydrogen bonded structure of water is sensitive to temperature.¹⁹ This makes the water–PEG interface an appropriate platform to study the contribution of hydration and diffusion on a solvolysis reaction.

In a recent study,²⁰ we have shown the explicit role of ultrafast solvation dynamics and the associated bound to free-type water transition to regulate the kinetics of benzoyl chloride solvolysis reaction in a reverse micellar (RM) interface. It was observed that the reaction at the RM interface follows an Arrhenius type activation energy barrier crossing model and the corresponding activation energy could be deconvoluted into two individual contributions coming from (i) the conversion of bound type water into the free type and (ii) nucleophilic attack of water. In continuation of this study, we extend our idea in the present communication to involve the role of diffusion of the water molecules through the polymer chain in a restricted environment of polymers as a nucleophile and its contribution to the overall reaction rate. Here, in order to explore the interaction of water molecules with a polymer chain, we measure the solvation dynamics of water using a fluorophore Coumarin 500 (C500), which is capable of monitoring the solvation at the polymer hydration region. C500 is sparingly soluble in water and remains either in bulk PEG or in the PEG–water interface. The choice of the probe lies on the fact that when excited at 409 nm, only the probe molecules residing at the interface and/or facing the water molecules get excited as has been observed in reverse micelles (RMs)^{21–23} and mixed solvents,²⁴ and hence provides the spectroscopic information from the water molecules at the PEG hydration region only. Also the BzCl solvolysis takes place only at the interface where water molecules act as the nucleophile. Thus the spectroscopic information coming from the C500 could be correlated with the solvolysis results as both the phenomena occur at the interface. From the temperature-dependent solvation dynamics studies, we estimate the energy barrier associated with the transition from bound to free type water molecules at the interface. The same activation energy is measured from acoustic and densimetric measurements, and the result is in good agreement with the solvation dynamics measurements. The temperature-dependent polarization gated fluorescence anisotropy of the probe monitors the microviscosity at the polymer hydration region. Microviscosity is the friction experienced by a solute (here the probe C500) at the microscopic scale and is an important parameter for characterizing the local environment as modest changes in the local viscosity lead to variable diffusion as well as chemical reaction rates. Kramers²⁵ formulated a kinetic model for reactions in which the reactants diffuse in the rate-limiting step,

and it was found that the time constant of the chemical reaction depends linearly on the viscosity of the medium. In a molecularly homogeneous solution, the local viscosity is equivalent to the macroviscosity. However, in polymeric solutions, where the solvent is markedly heterogeneous at the molecular level, the microviscosity differs significantly from the macroviscosity. Temperature-induced alteration of microviscosity can provide an idea of the activation energy associated with the diffusion of water molecules at the PEG surface. The energy barrier associated with the diffusion of the reactants is estimated from the temperature-dependent microviscosity applying Kramer's formulism.²⁶ The activation barriers estimated from the temperature-dependent solvation dynamics and microviscosity studies are correlated with that obtained from the solvolysis reaction.

Materials and Methods

PEG 400 (Poly(ethylene glycol), M_w (average molecular weight) = 400) was purchased from Sigma and was dried over vacuum at 110–120 °C. Benzoyl chloride (BzCl) was purchased from Merck. Coumarin 500 was a product of Exciton. The volume fraction of water (V_w) was varied from 0.0 to 0.2 by adding calculated amount of water to PEG followed by vigorous stirring. All the temperature-dependent studies were performed at a fixed $V_w = 0.05$. The kinetics of solvolysis of BzCl was measured in a Shimadzu UV-2450 spectrophotometer by monitoring the time dependent change in the absorbance of BzCl at 288 nm.²³ Steady-state absorption and emission were measured with a Shimadzu UV-2450 spectrophotometer and a Jobin Yvon Fluoromax-3 fluorimeter, respectively with a temperature controlled attachment from Julabo (Model: F32). Fluorescence transients were measured and fitted by using commercially available spectrophotometer (LifeSpec-ps) from Edinburgh Instrument, U.K. (excitation wavelength 409 nm, 80 ps instrument response function (IRF)) with a temperature controlled attachment from Julabo (Model: F32). The details of time-resolved measurements can be found in the Supporting Information. The time dependent fluorescence Stokes shifts, as estimated from TRES (time resolved emission spectroscopy), were used to construct the normalized spectral shift correlation function or the solvent correlation function $C(t)$ defined as

$$C(t) = \frac{\tilde{\nu}(t) - \tilde{\nu}(\infty)}{\tilde{\nu}(0) - \tilde{\nu}(\infty)} \quad (1)$$

where $\tilde{\nu}(0)$, $\tilde{\nu}(t)$, and $\tilde{\nu}(\infty)$ are the emission maxima (in cm^{-1}) at time zero, t , and infinity, respectively. The $C(t)$ function represents the temporal response of the solvent relaxation process, as occurs around the probe following its photo excitation and the associated change in the dipole moment. For anisotropy ($r(t)$) measurements, emission polarization is adjusted to be parallel or perpendicular to that of the excitation, and anisotropy is defined as

$$r(t) = \frac{[I_{para}(t) - GI_{perp}(t)]}{[I_{para}(t) + 2GI_{perp}(t)]} \quad (2)$$

G , the grating factor, was determined following long time tail matching technique.²⁷ Volume and compressibility of the mixtures were calculated using the density and sound velocity values

(16) Sasahara, K.; Sakurai, M.; Nitta, K. *Colloid Polym. Sci.* **1998**, *276*, 643–647.

(17) Branca, C.; Magazù, S.; Maisano, G.; Migliardo, F.; Migliardo, P.; Romeo, G. *J. Phys. Chem. B* **2002**, *106*, 10272–10276.

(18) Olender, R.; Nitzan, A. *J. Chem. Phys.* **1995**, *102*, 7180–7196.

(19) Bjoerling, M.; Karlstroem, G.; Linse, P. *J. Phys. Chem.* **1991**, *95*, 6706–6709.

(20) Verma, P. K.; Makhil, A.; Mitra, R. K.; Pal, S. K. *Phys. Chem. Chem. Phys.* **2009**, DOI:10.1039/B905573H.

(21) Majumder, P.; Sarkar, R.; Shaw, A. K.; Chakraborty, A.; Pal, S. K. *J. Colloid Interface Sci.* **2005**, *290*, 462–474.

(22) Mitra, R. K.; Sinha, S. S.; Pal, S. K. *Langmuir* **2008**, *24*, 49–56.

(23) Mitra, R. K.; Sinha, S. S.; Verma, P. K.; Pal, S. K. *J. Phys. Chem. B* **2008**, *112*, 12946–12953.

(24) Mitra, R. K.; Verma, P. K.; Pal, S. K. *J. Phys. Chem. B* **2009**, *113*, 4744–4750.

(25) Kramers, H. A. *Physica* **1940**, *7*, 284–304.

(26) Jacob, M.; Schindler, T.; Balbach, J.; Schmid, F. X. *Proc. Natl. Acad. Sci. U.S.A.* **1997**, *94*, 5622–5627.

(27) Lakowicz, J. R. *Principles of fluorescence spectroscopy*; Kluwer Academic/Plenum: New York, 1999.

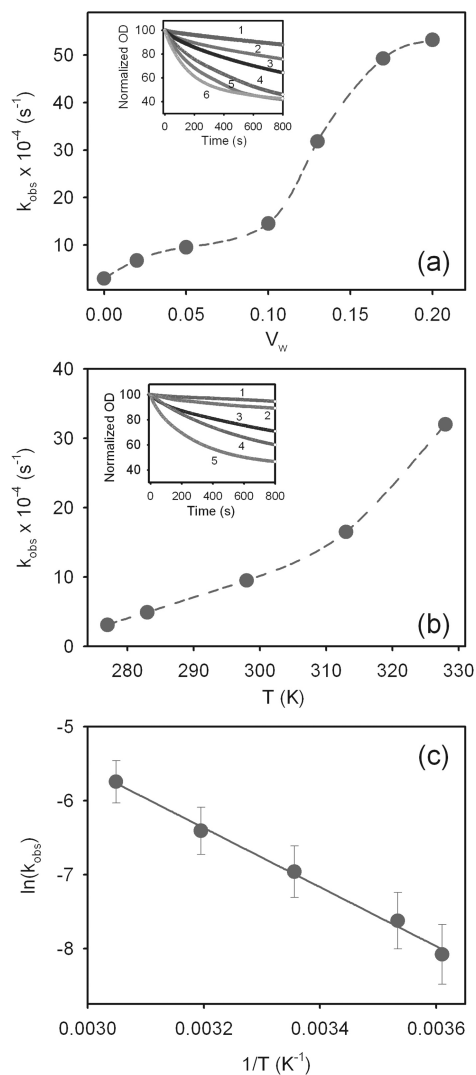


Figure 1. (a) Rate constant of solvolysis of BzCl in water-in-PEG mixture as a function of volume fraction of water (V_w) at 298 K. The broken line is a guide to the eye. The corresponding decay transients of BzCl absorption at different V_w are shown in the inset: (1) 0; (2) 0.02; (3) 0.05; (4) 0.10; (5) 0.13; (6) 0.2. (b) Rate constant of solvolysis of BzCl in water-in-PEG mixture as a function of temperature at $V_w = 0.05$. The broken line is a guide to the eye. The corresponding decay transients of BzCl absorption at different temperatures are shown in the inset: (1) 277 K; (2) 283 K; (3) 298 K; (4) 313 K; (5) 328 K. (c) Arrhenius plot $\ln(k_{\text{obs}})$ vs $1/T$ for temperature-dependent solvolysis of benzoyl chloride. The solid line is the linear fit.

measured by a density meter; model DSA5000 from Anton Parr (Austria) with an accuracy of $5 \times 10^{-6} \text{ g mL}^{-1}$ and 0.5 m s^{-1} in density and sound velocity measurements, respectively. The calculations for volume and compressibility determinations could be found in the Supporting Information.

Results and Discussion

As an initial approach toward the understanding of water reactivity near the PEG surface, we have studied the kinetics of solvolysis of BzCl at various volume fraction of water (V_w) in PEG. This solvolysis reaction is a well studied one and is reported to take place at the interface of the reverse micelle (RM) wherein the free interfacial water molecules act as the nucleophiles and the

Table 1. Rate Constants (k_{obs}) for Solvolysis of Benzoyl Chloride in Water-in-PEG Mixture at Various Volume Fractions of Water (V_w)

volume fraction of water (V_w)	$k_{\text{obs}} \times 10^{-4} \text{ (s}^{-1}\text{)}$
0.00	2.8
0.02	6.8
0.05	9.5
0.10	14.5
0.13	31.8
0.17	49.3
0.20	53.2

reaction follows a simple first order kinetics.^{23,28} Figure 1a depicts the rate of change of absorbance and the rate constants of solvolysis of BzCl at various V_w values. The observed rate constant (k_{obs}) of the solvolysis reaction as a function of V_w is given in Table 1. It is important to note that the values of k_{obs} are considerably smaller than that observed in bulk water ($k = 1.1 \text{ s}^{-1}$)²⁹ indicating that the water molecules are in highly restricted environment near the PEG surface resulting in their poor nucleophilic character similar to those encountered in RM systems.^{20,30} In mixtures of water-in-PEG, it is necessary to account for the attractive interactions (due to the hydrogen bond formation between water and ether oxygen of the PEG chain, and homomolecular hydrogen bonding), and repulsive interaction (between water and methylene unit of PEG). Near the PEG water interface (at very low concentration of water) the water-PEG hydrogen bond interaction predominates. Molecular dynamics simulation studies have established that there are at least two types of hydrogen bond present in the PEG-water system.⁵ Ethylene moiety acts as a scavenger for the water molecules as the first batch of water molecules are added to the PEG. The basic hydration of PEG is not satisfied until two water molecules have been added to each $-\text{CH}_2\text{CH}_2\text{O}-$ group and average number of water molecules associated with each ethylene unit is 2.9.⁵ So the reactivity of water in the water-PEG system can be modulated by altering the hydration structure. As can be observed from Table 1 and Figure 1a, k_{obs} increases first marginally and then considerably with increase in V_w to reach a constant value. At zero hydration the observed rate is due to the contribution from the polymeric hydration region containing EO chain and terminal OH group of the polymer toward the solvolysis process and the possibility of the presence of a trace amount of water as impurity. As water is added gradually into PEG, they are placed near the PEG chain by making rigid hydrogen bonding and thereby forming the layer of interfacial water molecules. As the fraction of interfacial free type water molecules increases the possibility to solvating the leaving group (here Cl^-) increases, which accelerates the solvation rate. Upon further addition of water, a bulk limit is reached and the rate of the reaction saturates (Figure 1a). Note that the value of k_{obs} in the present study (in the range of $6.8 \times 10^{-4} \text{ s}^{-1}$ to $53.2 \times 10^{-4} \text{ s}^{-1}$) is comparable with that observed in RMs (in the range of $4.0 \times 10^{-4} \text{ s}^{-1}$ to $41.6 \times 10^{-4} \text{ s}^{-1}$).²⁸ This supports the presence of interfacial type of water which can be exploited to modulate the hydration structure of the PEG-water system and the water reactivity in the water-PEG mixture in a manner similar to that in RMs by varying the amount of water.^{30,31}

At this point, it is important to consider the contribution of both the polymer chain and interfacial water in the total reaction kinetics, as it is observed that dry PEG also contribute to the

(29) Cabaleiro-Lago, C.; Garcia-Rio, L.; Herves, P.; Perez-Juste, J. *J. Phys. Chem. B* **2005**, *109*, 22614–22622.

(30) Garcia-Rio, L.; Leis, J. R.; Iglesias, E. *J. Phys. Chem.* **1995**, *99*, 12318–12326.

(31) Garcia-Rio, L.; Leis, J. R.; Moreira, J. A. *J. Am. Chem. Soc.* **2000**, *122*, 10325–10334.

(28) Garcia-Rio, L.; Leis, J. R.; Mejuto, J. C. *Langmuir* **2003**, *19*, 3190–3197.

solvolysis of BzCl. To evaluate the relative contribution of the polymer chain and the interfacial water, let us consider a simple model and assume that the observed kinetics has cumulative effect with individual contribution from both. At first, let us consider the distribution of the reactant (BzCl) between the polymer–water interfacial region associated with the EO chains and terminal OH groups (polymeric hydration region), and the water present at the interface according to the following,



where BzCl_h stands for the BzCl molecules present at the polymer hydration region and BzCl_w are those present in the close contact of the water molecules at the interface. The corresponding equilibrium constant K_{hw} is given as,

$$K_{hw} = \frac{[\text{BzCl}_w]}{[\text{BzCl}_h]} \quad (4)$$

Now assume that both BzCl_h and BzCl_w undergoes a first order solvolysis reaction individually with corresponding rate constants of k_h and k'_w , where k'_w could be related to the solvolysis rate constant in bulk like water (k_w) as, $k'_w = \alpha k_w$, where α is a fraction which tends to one as the interfacial water converts into the bulk type. If it is assumed that the observed concentration of BzCl is contribution from both BzCl_h and BzCl_w at any time t ,

$$[\text{BzCl}]_{\text{obs}} = [\text{BzCl}]_h + [\text{BzCl}]_w \quad (5)$$

then it can easily be shown that,

$$(1 + K_{hw}) \exp(-k_{\text{obs}}t) = \exp(-k_h t) + K_{hw} \exp(-k'_w t) \quad (6)$$

Now, we consider the relative contribution of k_h and k'_w toward k_{obs} from eq 6. It is observed from Table 1 that k_{obs} values are considerably higher than k_h , and eq 6 could hold true only if the first term has negligible contribution toward the total expression of the right-hand side. k'_w is in turn expected to be higher than k_{obs} , but the presence of the K_{12} term, which is much less than 1 due to the negligible solubility of BzCl in water, contributes mostly to the total expression. Note that k'_w is related to k_w with a fraction α , and as V_w increases, α also increases imparting to a higher value to k'_w , which in turn corresponds to a higher value of k_{obs} as expected from eq 6 and as experimentally evidenced (Table 1). On the other hand k_h has no dependency toward V_w and hence does not contribute to k_{obs} . In order to further strengthen our argument, we tried to fit the BzCl absorption decay biexponentially with a forced rate constant of $2.8 \times 10^{-4} \text{ s}^{-1}$ for the hydrated systems, and it was found that the fits were not good enough and also the contribution of the additional term toward the total fitting is very small. This contradicts our initial assumption that k_{obs} has an individual contribution from k_h and confirms that k_{obs} is predominantly controlled by the reaction kinetics of the interfacial water molecules.

It is worth mentioning here that the solvolysis of BzCl is reported to take place simultaneously in two different reaction channels in mixed solvents, namely the associative and the dissociative channel, and the crossover between these two mechanisms depend upon the composition of the mixed solvent.^{32–34} A similar phenomenon is also encountered in restricted media like

Table 2. Rate Constants (k_{obs}) for Solvolysis of Benzoyl Chloride in Water-in-PEG Mixture at Different Temperatures at $V_w = 0.05$

temperature (K)	$k_{\text{obs}} \times 10^{-4} (\text{s}^{-1})$
277	3.1
283	4.9
298	9.5
313	16.5
328	32.0

RMs wherein the crossover between the two mechanisms depend upon the water content in the RMs.^{28,29,31} It has been reported that in a restricted medium like AOT/isooctane RM, the reaction proceeds through an associative mechanism for less hydrated systems ($w_0 \leq 10$, where, $w_0 = [\text{water}]/[\text{AOT}]$), whereas in a hydrated system, the dissociative mechanism predominates. As the present system of water-in-PEG resembles an RM system, a similar analogy could also be followed here. As observed from Figure 1a, the reaction rate increases appreciably at $V_w \geq 0.5$ indicating a transition of the level of hydration and appearance of the free-type water in the system. In analogy with the RM system, the solvolysis reaction in this region could be assigned to be governed by the dissociative mechanism. To get further evidence we measure the emission spectra of C500 in this region and the observed peak at $\sim 500 \text{ nm}$ is in excellent agreement with that obtained in AOT/isooctane RM with $w_0 \geq 10$ system.²² This indicates that the water molecules in the water–PEG system at this level of hydration is equivalent to that in the RM system and as a first approximation the solvolysis reaction could be considered to follow a dissociative mechanism.

To have an insight on the energetics associated with the solvolysis reaction, we perform the temperature-dependent kinetic study of solvolysis of BzCl at $V_w = 0.05$. The choice of $V_w (= 0.05)$ lies on the fact that beyond this water concentration, further addition of water rapidly increases the rate of reaction (Figure 1a) indicating to the appearance of bulk-like water in the system. Since our prime interest of this work is to monitor the reaction dynamics at the interface, we prefer to monitor the experiment at low water concentration. Figure 1b shows the kinetics at different temperatures ranging from 278 to 343 K and the rate constants are presented in Table 2. It is evidenced from the table that increase in temperature accelerates the reaction. The increase in temperature lowers the PEG–water interaction strength; which is likely to be attributed to the enhanced thermal motions leading to lower residence times of water molecules in the rigidly bonded hydration layer of the polymer. The observed acceleration of k_{obs} is due to the increased fraction of interfacial free water molecules which eventually act as the nucleophile at higher temperature owing to the rupture of hydrogen bonds. The temperature dependence of k_{obs} is thus an effect arising out of the thermal contribution and rupture of loosely bound water molecules. The temperature dependency of k_{obs} can be used to calculate the overall activation energy needed for the reaction ($\Delta E_{\text{act}}^{\text{rcn}}$) following an Arrhenius model. $\ln(k_{\text{obs}})$, when plotted in an Arrhenius like model provides a good linear fit (Figure 1c) with activation energy value of $7.9 \pm 0.8 \text{ kcal mol}^{-1}$. This activation energy barrier is likely to be a cumulative effect of breaking and reforming of the intermolecular hydrogen bond and its realignment (or relocation) through diffusion. The relative contribution of both to the overall activation energy will be discussed in the subsequent sections.

Let us now concentrate on the dynamics of the water molecules at the PEG–water interface and find a possible correlation between water reactivity with its dynamics. Figure 2a shows the fluorescence transients of the probe C500 at 298 K at $V_w = 0.05$ at

(32) Bentley, T. W.; Koo, S. I. *J. Chem. Soc., Perkin Trans. 2* **1989**, 1385–1392.

(33) Bentley, T. W.; Koo, S. I. *J. Chem. Soc., Chem. Commun.* **1988**, 41–42.

(34) Bentley, T. W.; Llewellyn, G.; McAlister, J. A. *J. Org. Chem.* **1996**, 61, 7927–7932.

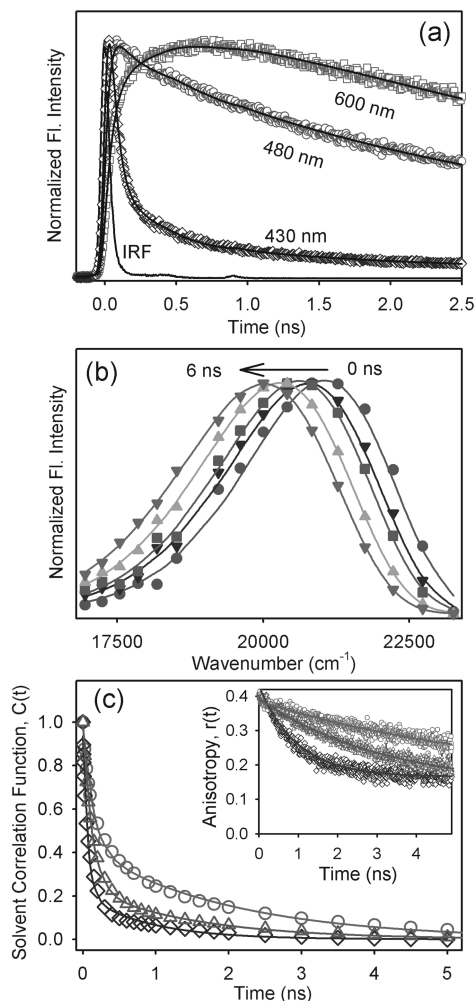


Figure 2. (a) Fluorescence decay transients of C500 at three different wavelengths in the water-in-PEG mixture at 298 K for volume fraction of water (V_w) = 0.05. (b) Time-resolved emission spectra (TRES) of C500 in water-in-PEG mixture at V_w = 0.05 at 278 K. (c) Solvent correlation function, $C(t)$, of C500 at different temperatures: (1) 277 K (circle); (2) 298 K (triangle); (3) 328 K (diamond). The corresponding time-resolved anisotropy decay, $r(t)$, are shown in the inset.

three selected wavelengths of 430, 480, and 600 nm, respectively. The transient at 430 nm (blue end of the emission spectrum) is fitted tetraexponentially with time components of 0.03 (80%), 0.17 (13%), 0.90 (4%), and 4.84 ns (3%). For the extreme red wavelength (600 nm), a distinct rise component of 0.55 ns is obtained along with a decay component of 5.0 ns. The presence of faster decay components at the blue end and a rise component at the red wavelength is consistent with the picture of solvation in the water-in-PEG system. As the temperature is increased to 328 K, the transients still show wavelength dependency, however, with a decrease in the time constants. Using the decay transients at different wavelengths, we construct the time-resolved emission spectra (TRES) at different temperatures. A representative TRES at 298 K for V_w = 0.05 is presented in Figure 2b. Figure 2c depicts the solvent correlation function ($C(t)$) at three different temperatures namely 278, 298, and 328 K. All these curves are well fitted biexponentially and the time constants are presented in Table 3. It is evident from the table that one of the solvation time constants is of the order of several hundreds of picoseconds, while the other is of the order of a few nanoseconds.

Table 3. Solvent Correlation and Rotational Time Constants for C500 in Water-in-PEG Mixture at Different Temperatures at V_w = 0.05

temperature (K)	τ_1 (ns)	τ_2 (ns)	$\langle\tau_s\rangle$ (ns)	f_r^a	$\langle\tau_r\rangle$ (ns)
277	0.14 (56%)	2.60 (44%)	0.96	0.41	6.65
283	0.16 (59%)	1.85 (41%)	0.85	0.41	4.80
298	0.13 (75%)	1.50 (25%)	0.47	0.40	2.90
313	0.08 (73%)	0.90 (27%)	0.30	0.35	1.75
328	0.07 (78%)	0.90 (22%)	0.26	0.34	1.15

^a f_r represents the fraction of Stokes shift recovered from our instrumental setup.

Solvation dynamics measurements in neat liquid PEG are available in literature. Sen et al.³⁵ reported an ultrafast component < 350 fs and a 2 ps component in a PEO-PPO-PEO triblock copolymer micelle using the fluorescence probe Coumarin 480. Argaman and Huppert³⁶ studied the solvation dynamics of Coumarin 153 in short chain ethylene glycol monoethers (n = 2–4) and found an ultrafast component of ~50 fs along with a 2 ps component. They ascribed these ultrafast components arising out of the interplay of intra- and intermolecular interactions in the polymer. Olander and Nitzan¹⁸ carried out a molecular dynamics simulation with a series of ethers of different molecular weights and found that the ultrafast component for all the ethers studied was same in amplitude and duration. They concluded that the ultrafast time component for ethers originates from damped solvent vibrations about inherent solvent structures and could not be considered as an inertial component of solvation. Using Raman-induced Kerr-effect spectroscopy, Castner and co-workers³⁷ measured the ultrafast solvent relaxation of liquid ethylene glycol and found that the ultrafast responses of the ethylene glycol and water are similar and attributed to the similarities in the hydrogen bonding properties of these two liquids. It should be pointed out here that, due to our instrumental limitation (IRF ~ 80 ps), we are unable to detect a considerable fraction of fluorescence signal, which is of the order of subpicosecond or a few picoseconds. We estimate the lost contribution by calculating the maximum frequency of the time-zero fluorescence spectra of C500 in PEG by the method proposed by Fee and Maroncelli.³⁸ The time zero spectrum here means a fluorescence spectrum prior to any solvent relaxation and is not the experimental time-zero fluorescence spectrum. The time-zero frequency of the fluorescence spectrum maximum, $\nu_{em}^p(0)$ can be calculated by the following equation:

$$\tilde{\nu}_{em}^p(0) = \tilde{\nu}_{abs}^p - [\tilde{\nu}_{abs}^{np} - \tilde{\nu}_{em}^{np}] \quad (7)$$

where $\tilde{\nu}_{abs}^p$, $\tilde{\nu}_{abs}^{np}$ and $\tilde{\nu}_{em}^{np}$ are the absorption peak in polar solvent, absorption peak in nonpolar solvent, and emission peak in nonpolar solvent, respectively. In the present study, we use cyclohexane as the nonpolar solvent with absorption and emission maxima of C500 at 360 and 410 nm, respectively. Water is used as the polar solvent in which C500 produces an absorption peak at 390 nm. We calculate a 59% and 66% loss in the dynamical Stokes shift at 277 and 328 K, respectively (Table 3). Note that this lost signal belongs to the ultrafast solvation component, which arises out of the polymer chain relaxation and is not associated with the water dynamics in the confined environment. The essence of the present work lies on the correlation between the dynamics and energetics of bound to free-type

(35) Sen, P.; Ghosh, S.; Sahu, K.; Mondal, S. K.; Roy, D.; Bhattacharyya, K. *J. Chem. Phys.* **2006**, *124*, 204905–204913.

(36) Argaman, R.; Huppert, D. *J. Phys. Chem. A* **1998**, *102*, 6215–6219.

(37) Chang, Y. J.; Castner, J. E. W. *J. Chem. Phys.* **1993**, *99*, 7289.

(38) Fee, R. S.; Maroncelli, M. *Chem. Phys.* **1994**, *183*, 235–247.

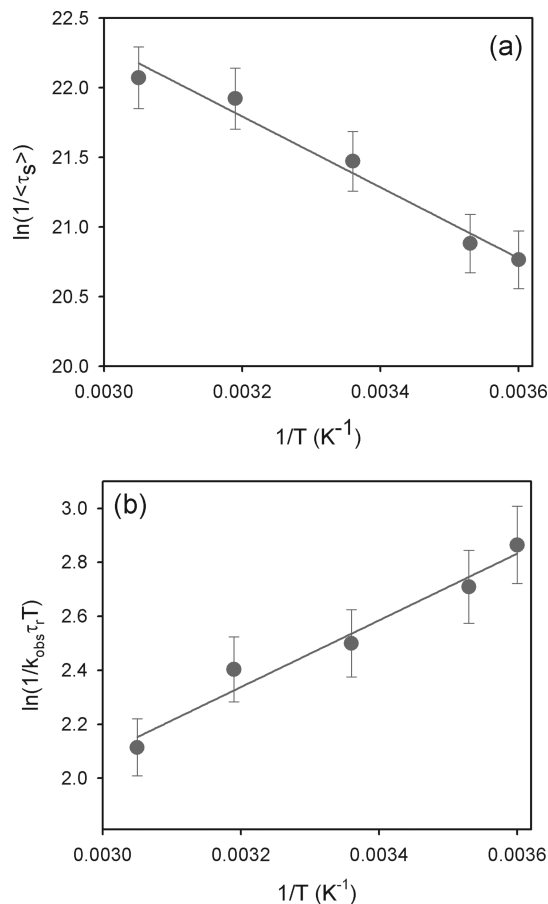


Figure 3. (a) Arrhenius plot $\ln(1/\langle\tau_{\text{solvation}}\rangle)$ vs $1/T$ with linear fit for temperature-dependent study of solvation dynamics. (b) Plot of $\ln(1/k_{\text{obs}}\tau_r T)$ vs $1/T$ with linear fit.

water transition with the overall reaction kinetics, and thus our discussion will remain meaningful if made on the slow time components recovered from the interfacial slow moving water molecules detectable with our TCSPC setup. As evidenced from Table 3, we obtain two slow components of ~ 100 and ~ 1500 ps, similar to those obtained by solvation dynamics measurements,^{36,39–42} Brillouin scattering measurements,^{43,44} dielectric measurements^{45,46} and these slow components are assigned as a contribution from the segmental motions of the polymer molecule and interconversion of bound and free water molecules. Such slow components are comparable with those reported earlier for water in restricted environments like aqueous

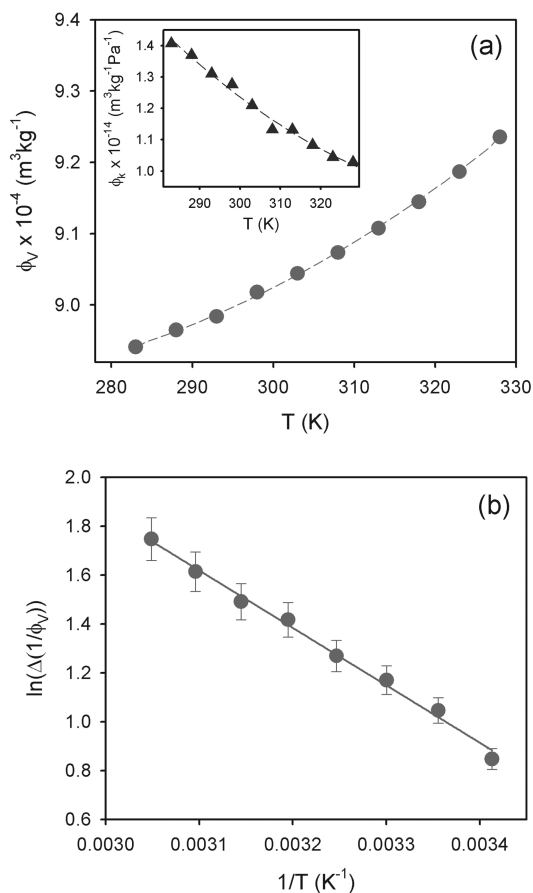


Figure 4. (a) Apparent specific volume (ϕ_v) of water in water-in-PEG mixture as a function of temperature with $V_w = 0.05$. The corresponding partial apparent adiabatic compressibility (ϕ_k) are shown in the inset. The broken lines are guide to the eyes. (b) Plot of $\ln(\Delta(1/\phi_v))$ vs $1/T$ with linear fit.

polymer solutions,⁴¹ micelles,^{47,48} and RMs.^{22,49–51} The overall decrease in the average solvation time constant, $\langle\tau_s\rangle$ ($\langle\tau_s\rangle = a_1\tau_1 + a_2\tau_2$) with increasing temperature, as evidenced from Table 3, reveals that an increase in temperature accelerates the solvation process. Note that at low temperature the polymer–water interaction is stabilized by both the primary hydration shell (hydrogen bonds between water molecules and ether oxygen) and the secondary hydration shell (hydrogen bonding between water molecules and terminal OH groups). As the temperature increases, the loosely bound water molecules become free resulting in a lower residence time of the water molecules in the hydration shell of the polymer, which perhaps accelerates the dynamics of water molecules.

The temperature-induced acceleration of the solvation dynamics of water in PEG mixture can be explained with the help of the multishell continuum model proposed by Bagchi et al. for structured water in micellar and protein surfaces.^{52–55} In this model the free energy difference for the dynamical exchange between free and bound water molecules is assumed to depend on the slow component of relaxation. The energetic of the exchange process depends upon the strength and the number of hydrogen bonded water molecules at the PEG interface. The temperature-induced bound to free type transition of water molecules is

(39) Shirota, H.; Segawa, H. *J. Phys. Chem. A* **2003**, *107*, 3719–3727.

(40) Pant, D.; Levinger, N. E. *Langmuir* **2000**, *16*, 10123–10130.

(41) Frauchiger, L.; Shirota, H.; Uhrich, K. E.; Castner, E. W. *J. Phys. Chem. B* **2002**, *106*, 7463–7468.

(42) Sen, S.; Sukul, D.; Dutta, P.; Bhattacharyya, K. *J. Phys. Chem. B* **2002**, *106*, 3763–3769.

(43) Lin, Y.-H.; Wang, C. H. *J. Chem. Phys.* **1978**, *69*, 1546–1552.

(44) Wang, C. H.; Li, B. Y.; Rendell, R. W.; Ngai, K. L. *J. Non-Cryst. Solids* **1991**, *131–133*, 870–876.

(45) Kaatz, U.; Kettler, M.; Pottel, R. *J. Phys. Chem.* **1996**, *100*, 2360–2366.

(46) Sato, T. N.; H.; Chiba, A.; Nozaki, R. *J. Chem. Phys.* **1998**, *108*, 4138–4147.

(47) Hara, K.; Kuwabara, H.; Kajimoto, O. *J. Phys. Chem. A* **2001**, *105*, 7174–7179.

(48) Balasubramanian, S.; Pal, S.; Bagchi, B. *Phys. Rev. Lett.* **2002**, *89*, 115505–115509.

(49) Corbeil, E. M.; Riter, R. E.; Levinger, N. E. *J. Phys. Chem. B* **2004**, *108*, 10777–10784.

(50) Dutta, P.; Sen, P.; Mukherjee, S.; Halder, A.; Bhattacharyya, K. *J. Phys. Chem. B* **2003**, *107*, 10815–10822.

(51) Sarkar, N.; Das, K.; Datta, A.; Das, S.; Bhattacharyya, K. *J. Phys. Chem.* **1996**, *100*, 10523–10527.

(52) Nandi, N.; Bagchi, B. *J. Phys. Chem. B* **1997**, *101*, 10954–10961.

(53) Nandi, N.; Bagchi, B. *J. Phys. Chem. A* **1998**, *102*, 8217–8221.

(54) Bhattacharyya, K.; Bagchi, B. *J. Phys. Chem. A* **2000**, *104*, 10603–10613.

(55) Nandi, N.; Bhattacharyya, K.; Bagchi, B. *Chem. Rev.* **2000**, *100*, 2013–2045.

assumed to be governed by an Arrhenius type of activation energy barrier crossing model.^{56–58} We plot $\ln(1/\langle\tau_s\rangle)$ vs $1/T$, which produces a good linear fit (Figure 3a) with corresponding activation energy ($\Delta E_{\text{act}}^{\text{soliv}}$) value of $5.0 \pm 0.5 \text{ kcal mol}^{-1}$. Note that the $\Delta E_{\text{act}}^{\text{soliv}}$ value is of the same order of magnitude to that obtained for the transition from bound type water (hydrogen bonded to polar headgroup) to free type water (not directly hydrogen bonded to headgroup) at the RM and micellar interface.^{20,22,56,58,59} This comparable value is a direct consequence of the dynamic nature of the primary and secondary hydration shell near the PEG surface which in turn is largely influenced by temperature. It is to be noted that C500 is sparingly soluble in water and therefore resides mainly at the surface of the PEG chain, and thus can precisely report the $\Delta E_{\text{act}}^{\text{soliv}}$ values occurring in the vicinity of the PEG chain.

The intermolecular bonds of water molecules at the PEG surface make the interfacial water molecules physically different from the bulk molecules, which induces considerable change in the apparent specific volume and adiabatic compressibility of water molecules due to their location.^{23,60,61} We measure the apparent specific volume (ϕ_v) and partial apparent adiabatic compressibility (ϕ_k) of water at different temperatures (Figure 4). As can be observed from the figure, ϕ_v increases, whereas ϕ_k decreases with temperature. An increase in ϕ_v indicates that the water molecules are approaching toward the bulk limit of specific volume of $10^{-3} \text{ kg m}^{-3}$, i.e. the interfacial hydration bonded water molecules get converted into bulk one at elevated temperature. A similar conclusion can be drawn with the increase in ϕ_k with temperature as water molecules are getting less strongly hydrogen bonded at higher temperature. This observation is in accordance with the earlier studies of Faraone et al.¹² wherein hydration number of PEG 600 decreases from ~ 34 to ~ 26 on increasing the temperature from 15 to 80 °C. In the present system, as we are using PEG as the solvent, with low concentration of water as the solute, a rough estimate could be made on the hydration state at the PEG surface by assuming that ϕ_v is related to the water molecules associated with the PEG surface. It could be argued that as the bound type water changes into bulk type, ϕ_v increases. Hence ϕ_v has an inverse relationship with the hydration number at the PEG surface and the change in the hydration number (Δn_h) is related to ϕ_v as follows:

$$\Delta n_h \propto \Delta(1/\phi_v) \quad (8)$$

If the bound to free water transition is associated with an activation energy ΔE_{act}^h then according to Arrhenius relation one can have, $\Delta n_h \propto \exp(\Delta E_{\text{act}}^h/RT)$, which in turn reduces to,

$$\Delta(1/\phi_v) \propto \exp(\Delta E_{\text{act}}^h/RT) \quad (9)$$

When $\ln(\Delta 1/\phi_v)$ is plotted against $1/T$, a good linear fit is obtained (Figure 4b) and the corresponding activation energy obtained is $4.7 \pm 0.4 \text{ kcal mol}^{-1}$, which is in excellent agreement with that obtained from our solvation dynamics studies ($5.0 \text{ kcal mol}^{-1}$). Thus the acoustic and densimetric study accords with the solvation dynamics study and supports the bound to free type water transition to be the responsible factor for the increased rate constant of solvolysis at higher temperature (Figure 1b).

It is to be noted that the observed $\Delta E_{\text{act}}^{\text{soliv}}$ value is smaller than the $\Delta E_{\text{act}}^{\text{rcn}}$ value. As has been discussed earlier, $\Delta E_{\text{act}}^{\text{rcn}}$ is a cumulative contribution from hydration and diffusion of nucleophilic water molecules. The solvation dynamics study gives an idea of the energy associated with the hydration process. Let us now find out the contribution from diffusion process. First we make an idea of the diffusion coefficient (D) of water molecules near the PEG surface at room temperature. The magnitude of diffusion coefficient (D) is directly related to the rms distance $\langle z^2 \rangle^{1/2}$ traveled by the species in time t by the relation,

$$\langle z^2 \rangle = 2Dt \quad (10)$$

For the present system, $\langle z^2 \rangle^{1/2}$ can be assumed to be the thickness of the bound water layer and at room temperature it is about 3.3 \AA . If t is taken to be the slowest solvation correlation time constant (1.5 ns in this case), then D has a value of $3.6 \times 10^{-11} \text{ m}^2 \text{ s}^{-1}$. This value is order of magnitude smaller than that of pure water ($\sim 10^{-9} \text{ m}^2 \text{ s}^{-1}$), micelle ($5 \times 10^{-9} \text{ m}^2 \text{ s}^{-1}$),⁶² and of the same order of magnitude as in RMs^{63–65} and other polymer solutions.^{5,12} Thus the water molecules in the vicinity of the PEG chain are highly structured and slow diffusing.

To get an idea on the temperature mediated modification of the water diffusion, we measure the temporal anisotropy decay, $r(t)$ of the probe in the water–PEG system at $V_w = 0.05$ at different temperatures (inset of Figure 2c). The rotational correlation time constants (τ_r) at different temperatures are given in Table 3. The decay transients are fitted single-exponentially along with a considerable offset value which perhaps signifies the overall tumbling or reorientation of the entire PEG chain. The value of the rotational time constant is of the order of a few ns confirming that the probe is at the interface of the PEG chain. The water molecules near the PEG chain are highly structured and an increase in temperature perturbs it making the reorientation time constant (τ_r) faster. According to Kramers' theory,^{25,26} a widely used concept in protein kinetics²⁶ and photoisomerisation processes,⁶⁶ the time constant of a chemical reaction in adiabatic condition depends on the diffusion in the solvent according to the following relation,

$$\tau_{\text{rcn}} \propto \eta \exp(\Delta E_{\text{act}}^{\text{diff}}/RT) \quad (11)$$

where the viscosity term and the activation energy barrier ($\Delta E_{\text{act}}^{\text{diff}}$) are associated with the diffusion process. The η term in eq 11 can be identified with the microviscosity experienced by the probe molecule in the PEG surface and can be equated to τ_r according to the Debye–Stokes–Einstein equation,

$$\tau_r = \frac{\eta V}{k_B T} \quad (12)$$

where, V is the volume of the probe molecule. Thus eq 11 takes up the form,

$$\tau_{\text{rcn}} \approx \frac{1}{k_{\text{obs}}} \propto \frac{k_B T \tau_r}{V} \exp(\Delta E_{\text{act}}^{\text{diff}}/RT) \quad (13)$$

(56) Mitra, R. K.; Sinha, S. S.; Pal, S. K. *J. Phys. Chem. B* **2007**, *111*, 7577–7583.

(57) Bhattacharyya, K. *Chem. Commun.* **2008**, 2848–2857.

(58) Pal, S.; Balasubramanian, S.; Bagchi, B. *J. Phys. Chem. B* **2003**, *107*, 5194–5202.

(59) Mitra, R. K.; Sinha, S. S.; Pal, S. K. *J. Phys. Chem. B* **2007**, *111*, 7577–7581.

(60) Amararene, A.; Gindre, M.; Le Huerou, J.-Y.; Nicot, C.; Urbach, W.; Waks, M. *J. Phys. Chem. B* **1997**, *101*, 10751–10756.

(61) Mitra, R. K.; Sinha, S. S.; Pal, S. K. *Langmuir* **2007**, *23*, 10224–10229.

(62) Bruce, C. D.; Senapati, S.; Berkowitz, M. L.; Perera, L.; Forbes, M. D. E. *J. Phys. Chem. B* **2002**, *106*, 10902–10907.

(63) Texter, J.; Antalek, B.; Williams, A. J. *J. Chem. Phys.* **1997**, *106*, 7869–7872.

(64) Feldman, Y.; Kozlovich, N.; Nir, I.; Archipov, N. G. V.; Zuev, Z. I. Y.; Fedotov, V. *J. Phys. Chem.* **1996**, *100*, 3745–3748.

(65) Schwartz, L. J.; DeCiantis, C. L.; Chapman, S.; Kelley, B. K.; Hornak, J. P. *Langmuir* **1999**, *15*, 5461–5466.

(66) Schneidera, S.; Brema, B.; Jägera, W.; Rehabela, H.; Lenoir, D.; Frankb, R. *Chem. Phys. Lett.* **1999**, *308*, 211–217.

Assuming that V does not change appreciably over the studied range of temperature, we get,

$$\left(\frac{1}{k_{\text{obs}}\tau_r T}\right) \propto \exp(\Delta E_{\text{act}}^{\text{diff}}/RT) \quad (14)$$

We plot $(1/k_{\text{obs}}\tau_r T)$ vs $1/T$ and a good linear fit is obtained (Figure 3b) and from the slope we calculate $\Delta E_{\text{act}}^{\text{diff}}$ to be $2.4 \pm 0.2 \text{ kcal mol}^{-1}$.

Let us now correlate the overall observation. The water structure near the PEG chain is rigid and is composed of hydration shell (consisting of two types of hydrogen bonding). For solvolysis to take place at the interface, the interfacial water molecules would need to reorient themselves to minimize their energy. However, reorientation would require breaking of hydrogen bond (with ether oxygen or terminal OH group of PEG chain) and reformation of hydrogen bond. This involves not only breaking and formation of hydrogen bonds but also rotation and migration of water molecules near the surface and also the breathing motion of the polymer chain. Note that the rigid network of water molecules at the PEG surface reduces their translational freedom resulting in its small diffusion coefficient.^{5,12} Thus solvolysis reaction is dependent on both hydration and diffusion of water molecules near PEG. The hydration barrier is manifested from the solvation dynamics studies and reorientation (diffusion) barrier is calculated applying Kramers model. Addition of these two barriers ($5.0 + 2.4 = 7.4 \text{ kcal mol}^{-1}$) is in excellent agreement with the overall activation energy ($7.9 \text{ kcal mol}^{-1}$) for the reaction.

Conclusions

Our report explores the water reactivity in PEG surface of water-in-PEG system. The temperature-dependent solvolysis

of BzCl gives an idea of the overall activation energy barrier of solvolysis reaction. The observed acceleration of rate constant supports the general view that the mobility of the water molecules near PEG increases with temperature due to rupture of loosely bound water molecules and thereby increasing the availability of interfacial water molecules. Applying Arrhenius model to the solvation dynamics of water we found activation energy to be of the order of 5 kcal mol^{-1} which is responsible for the exchange of bound to free type interfacial water molecules. This result is confirmed from temperature-dependent densimetric and acoustic studies. The temperature-dependent rotational anisotropy study also provides activation energy due to the diffusive motion as the probe experiences less microviscosity at elevated temperature due to decreased residence time of the water molecules at the PEG surface. These two energy values sum up to be in excellent agreement with the overall reaction activation energy. In solvolysis, the water molecules need to undergo a reaction which involves two energy barriers which are attributed to the formation and availability of free water molecules at the interface and diffusion of those. Our study confirms the relative contribution of both hydration and diffusion to the total reaction.

Acknowledgment. P.K.V. thanks the CSIR for fellowship. We thank the DST for financial support (SR/SO/BB-15/2007).

Supporting Information Available: Text describing the time resolved fluorescence and acoustic and densimetric measurements. This material is available free of charge via the Internet at <http://pubs.acs.org>.